Statistical characteristics of seismo-ionospheric GPS TEC disturbances prior to global Mw ≥ 5.0 earthquakes (1998–2014)

Munawar Shah [a,c], Shuanggen Jin [a,b,*]

[a] Shanghai Astronomical Observatory, Chinese Academy of Sciences, Shanghai 200030, China
[b] Department of Geomatics Engineering, Bulent Ecevit University, Zonguldak 67100, Turkey
[c] University of Chinese Academy of Sciences, Beijing 100047, China

ARTICLE INFO

ABSTRACT

Pre-earthquake ionospheric anomalies are still challenging and unclear to obtain and understand, particularly for different earthquake magnitudes and focal depths as well as types of fault. In this paper, the seismo-ionospheric disturbances (SID) related to global earthquakes with 1492 Mw ≥ 5.0 from 1998 to 2014 are investigated using the total electron content (TEC) of GPS global ionosphere maps (GIM). Statistical analysis of 10-day TEC data before global Mw ≥ 5.0 earthquakes shows significant enhancement 5 days before an earthquake of Mw ≥ 6.0 at a 95% confidence level. Earthquakes with a focal depth of less than 60 km and Mw ≥ 6.0 are presumably the root of deviation in the ionospheric TEC because earthquake breeding zones have gigantic quantities of energy at shallower focal depths. Increased anomalous TEC is recorded in cumulative percentages beyond Mw = 5.5. Sharpness in cumulative percentages is evident in seismo-ionospheric disturbance prior to Mw ≥ 6.0 earthquakes. Seismo-ionospheric disturbances related to strike slip and thrust earthquakes are noticeable for magnitude Mw6.0–7.0 earthquakes. The relative values reveal high ratios (up to 2) and low ratios (up to −0.5) within 5 days prior to global earthquakes for positive and negative anomalies. The anomalous patterns in TEC related to earthquakes are possibly due to the coupling of high amounts of energy from earthquake breeding zones of higher magnitude and shallower focal depth.

1. Introduction

Seismic events cause widespread loss of infrastructure and lives. In the modern era scientists are trying to combat these hazards in order to protect humans and buildings. GPS TEC can provide some insight into seismo-ionospheric disturbances related to seismic events (Afraimovich et al., 2010; Jin et al., 2010). A number of publications report that seismo-ionospheric disturbances (SID) are caused by a large amount of energy released into the ionosphere from earthquake preparation zones. Variations in TEC, foF2 and NmF2 have correlated with large amounts of energy released during the earthquake preparation period, which are probably signs of a forthcoming large magnitude earthquake (Bolt, 1999; Freund, 2000; Singh et al., 2010; Jin et al., 2013). The radon emission from the Earth's crust in an earthquake preparation zone causes changes in the atmosphere, especially the ionosphere

(Jin et al., 2011). The moderate correlation between earthquakes and foF2 of ionosonde stations is termed as a seismo-ionospheric disturbance related to forthcoming earthquakes (Gwal et al., 2011). The statistical analysis of seismo-ionospheric TEC disturbances related to earthquakes in Taiwan showed that the TEC anomaly appears frequently 5 days before the earthquake and an increased TEC has been observed in the afternoon period 3 days prior to the earthquake (Liu et al., 2000). Similarly statistical analysis and case studies for earthquakes in Japan during 1998–2010 reveal that seismo-ionospheric disturbances related to a shallow hypocenter cause disturbances in TEC as compared to deep hypocenter earthquakes (Liu et al., 2006; Kon et al., 2011; Lin, 2013). Interpreted results of TEC in North America showed that seismo-ionospheric disturbances on the continent was due to forthcoming earthquakes and sharpness in TEC increased with increasing magnitude as well as precursory alarm of the coming earthquake (Sardon et al., 1994; Molchanov and Hayakawa, 2002; Zolotov et al., 2012). The seismo-ionospheric disturbance significantly decreases after the main shock and the after effect of seismo-ionospheric disturbances is studied with detail and modeled in different ways to explain the behavior of seismo-ionospheric anomalies related to seismic

* Corresponding author at: Shanghai Astronomical Observatory, Chinese Academy of Sciences, Shanghai 200030, China.
   E-mail addresses: sgjin@shao.ac.cn, sg.jin@yahoo.com (S. Jin).

activity (Jin et al., 2014, 2015; Pradipta et al., 2014). Analysis for threshold and different types of faults also show that disturbances in TEC can be seen for strike slip faults with some explanations of the abnormality related to larger Richter scale earthquakes (Fatkullin et al., 1989; Pulinets et al., 1991; Astafyeva et al., 2014).

Le et al. (2011) statistically studied anomalies in the GIM TEC prior to 736 Mw ≥ 6.0 worldwide earthquakes during 2002–2010 and found that the frequency of increases and decreases in SIPs is proportional to the magnitude, but inversely related to depth and day of the forthcoming earthquake. Their results suggest the effect of latitudinal enhancement in TEC, which is due to the fact that large amount of energy was transmitted into the atmosphere before the main shock of a larger earthquake than a smaller earthquake. But for small magnitudes like Mw ≤ 6.0, the seismo-ionospheric anomalies in TEC related to earthquake breeding zone are less obvious than the large magnitude earthquake. Similarly, Kon et al. (2011) conducted a statistical analysis and showed that dissimilarities in TEC in Japan during 1998–2010 tend to appear 1–5 days before earthquakes, and positive anomalies tend to be more prominent than negative anomalies all over Japan. The seismo-ionospheric precursory mechanism was discussed in a model, which showed a lithosphere–atmosphere–ionosphere coupling and explained the disturbance in the ionosphere caused by seismic events (Pulinets and Ouzounov, 2011). The TEC has variability influenced by large magnitudes and shallow depth earthquakes, which is a strong contributor of disturbance in the sensitive F2 layer of the ionosphere. Seismo-ionospheric disturbances 40 days before (after) the 2008 Wenchuan earthquake were observed statistically and the suspected seismo-ionospheric disturbance related to Mw = 7.9 Wenchuan in TEC was found at UT = 04:00. This variation was also observed in CHAMP (N_e) and DEMETER satellite data for the same days (Ryu et al., 2014). However, seismo-ionospheric anomalies prior to earthquakes are still challenging and unclear, particularly for different earthquake magnitudes and types of fault (Jin et al., 2007a). In this paper, a statistical analysis of pre-earthquake ionospheric disturbances related to the global earthquakes of Mw ≥ 5.0 during 1998–2014 is studied from global GIM TEC, including different earthquake sources worldwide as well as diverse magnitudes and depths.

2. GPS TEC and earthquakes

Now dual-frequency GPS observations can estimate the ionospheric TEC and its variations (e.g., Jin et al., 2004, 2007b, 2008). We used the TEC data of GPS global ionosphere maps (GIM) (ftp://cddisa.gsfc.nasa.gov/pub/gps/products/ionex). TEC data from GPS ionex have a 2-h temporal resolution and a spatial resolution of 2.5° × 5° in latitude and longitude (Schaer and Krankowski, 2009). In our study, TEC data from IGS GIM are used for statistical analysis and investigating spatial variations of seismo-ionospheric disturbances. We extracted the TEC data from GPS ionex during 1998–2014 for global earthquakes of Mw ≥ 5.0 and investigated the seismo-ionospheric variations in TEC prior to the earthquake. TEC is expressed in TEC unit (TECU) where 1 TECU = 10^{16} electron/m^2. More GIM TEC information and recent improvements were given and discussed (Hernandez-Pajares et al., 1999). The earthquake database and fault catalogs were obtained from the USGS earthquakes archive (http://earthquake.usgs.gov/earthquakes/search/). The solar wind condition and geomagnetic indices data were obtained from NASA satellites (http://omniweb.gsfc.nasa.gov) and Kiyoto University (http://wdc.kugi.kyoto-u.ac.jp/kp).

Fig. 1 illustrates the location of earthquakes with geographic latitude and longitude. The earthquake catalogs of USGS in Taiwan and Japan are used to accurately study worldwide earthquake occurrences. The magnitude is denoted by the circle size. The earthquakes shown in Fig. 1 were not severely affected by the geomagnetic storm. 492 Mw ≥ 5.0 earthquakes during 1998–2014 were studied excluding the earthquakes whose 10 days fall near the geomagnetic storm of a higher scale (Dst ≤ −50 nT). According to Gutenberg and Richter (1956), large amounts of energy are released with a higher magnitude and seismic energy and the difference between two magnitudes of earthquake is 10 times. For example, Fig. 2 shows the geomagnetic condition for a Mw = 6.6 Siberian (Russia) earthquake on 27 December 2011 with latitude 56.84°N, longitude 95.91°E and depth 15.0 km, including solar wind and geomagnetic indices for 10 days before this large magnitude earthquake. We were interested in the geomagnetic condition 10 days before the Mw = 6.6 earthquake without enhancement in the geomagnetic index. The fluctuation in geomagnetic indices is due
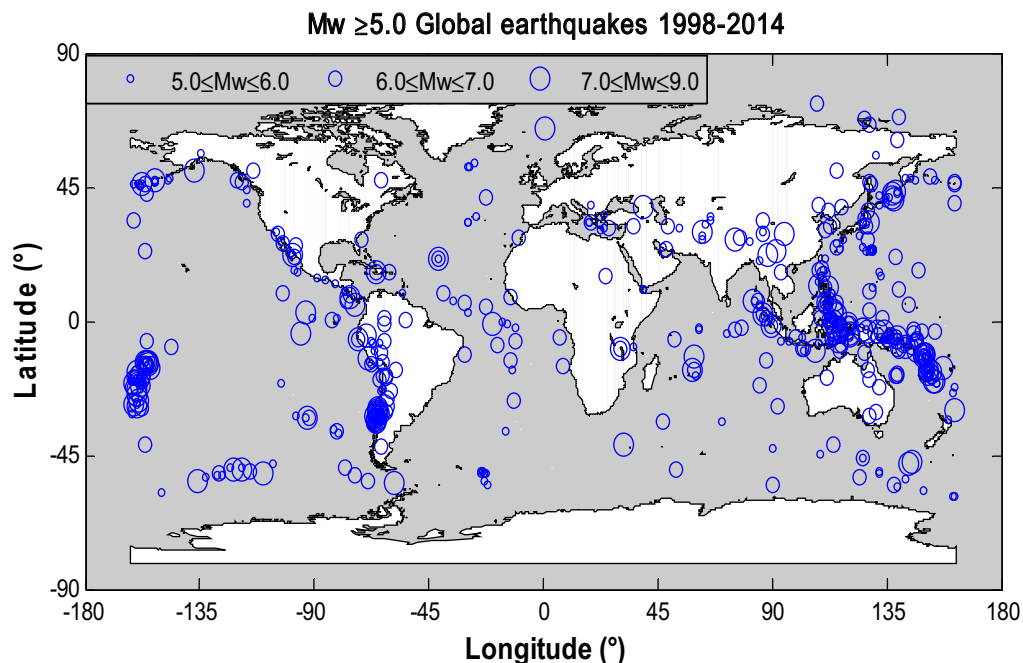

Fig. 1. Distribution of global Mw ≥ 5.0 earthquakes during 1998–2014. The size circle represents the magnitude.
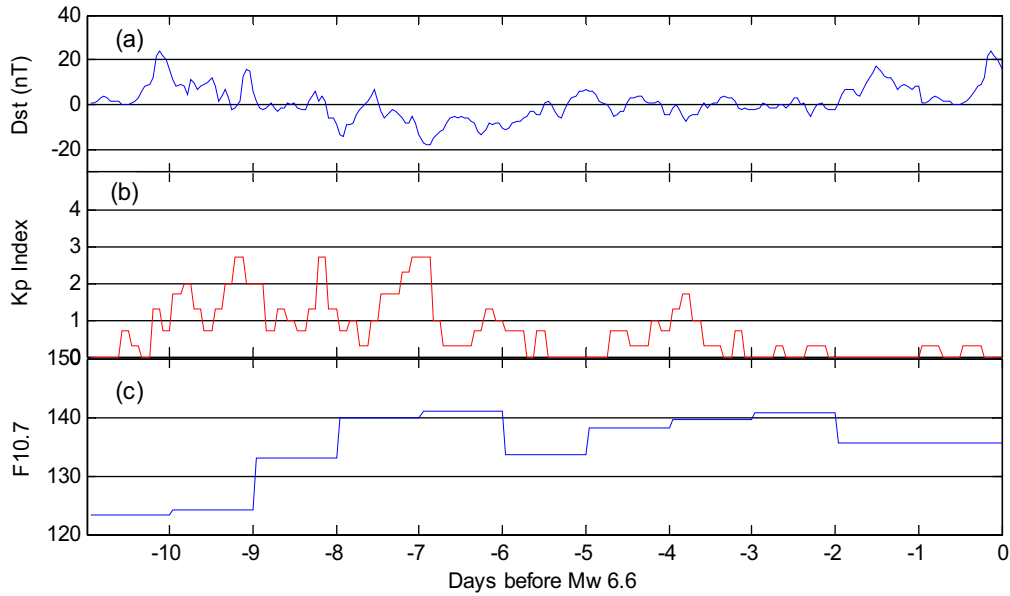
Fig. 2. 10-day conditions of (a) Dst(nT), (b) Kp index and (c) F10.7 (solar flux) before the 2011 Mw6.6 Siberia (Russia) earthquake.

to strong solar winds and the high value of Dst (nT) that can be seen as high level of disturbance for long time (Tsurutani and Gonzalez, 1987). Disturbances in the ionosphere with sources other than earthquakes and geomagnetic activities were discussed by Fejer and Scherliess (1995).

3. Statistical method

The statistical method was used for detecting seismo-ionospheric disturbance related to earthquakes. To observe deviation of abnormal signals, the 10-day before (after) successive mean ⟨TEC⟩ and standard deviation (σ) for every 2 h of TEC for the period 1998–2014 were calculated. An increment (decline) on the 11th day and the preceding 10 days was noted. Further to confirm the 95% deviation of TEC, we calculated the 95% confidence bound for TEC in the desired period. We omitted other earthquakes in these 10 days as well as the days following the magnetic storm. To calculate the standard error (SE), the standard deviation is divided by the square root of the number of two-hourly TEC in successive 10 days from the time of study. Since the number of two-hourly TEC in successive 10 days was 120, the value of z-percentile at $\alpha = 0.05$ significance level is 1.96. We computed the $Z_{1-\alpha/2}$ percentile for degree of freedom (df) of the number of two-hourly TEC in 10 days. This percentile was used to calculate the upper and lower confidence intervals. For the normal distribution of mean ⟨TEC⟩ and standard deviation (σ), the concept of t-distribution for TEC was developed.

$$T_{n-1} = \frac{\langle \text{TEC} \rangle - \sigma}{\text{SE}} \tag{1}$$

where ⟨TEC⟩ is the mean of two-hourly TEC data in 10 days from the time of study, σ is standard deviation and SE (standard error) is equal to $\sigma/\sqrt{(n)}$, and n is number of two-hourly TEC for 10 days. Now t-distribution for number of two-hourly TEC in 10 days at $1 - \alpha/2$ significance level is

$$T_{n-1}(t) = \frac{1-\alpha}{2} \quad \rightarrow t_{df, 1-\alpha/2} \tag{2}$$

Use Eq. (2) for TEC to construct the 95% upper and lower confidence level of Eq. (1).

$$-t_{df, 1-a/2} \left\langle \frac{\langle \text{TEC} \rangle - \sigma}{\text{SE}} \right\rangle + t_{df, 1-\alpha/2} \quad \text{or} \quad \langle \text{TEC} \rangle$$

$$- t_{df, 1-\alpha/2} * SE \langle \sigma \rangle \langle \text{TEC} \rangle + t_{df, 1-a/2} * SE \tag{3}$$

Since the number of two-hourly TEC in successive 10 days from the day of study was 120 h, the deviation from normal distribution of ⟨TEC⟩ and σ at $1 - \alpha/2$ for t-distribution was significantly small. However, the deviation for z-distribution was large. Therefore we used z-percentile in Eq. (3) instead of t-percentile for larger deviation from the normal distribution. In this study, we used z-distribution for $1 - \alpha/2$ percentile to observe a clear TEC anomaly. The 95% confidence bound for $n = 120$ with $df = n - 1$ in z-distribution is 1.96. After using z-percentile, Eq. (3) becomes

$$\langle \text{TEC} \rangle - z_{df, 1-\alpha/2} * SE \langle \sigma \rangle \langle \text{TEC} \rangle + z_{df, 1-\alpha/2} * SE \tag{4}$$

Thus when an observed TEC on some day increases (decreases) than previous 10 days $\langle \text{TEC} \rangle \pm z_{df, 1-\alpha/2} * SE$ by more than value of threshold, which is defined as seismo-ionospheric disturbance related to the earthquake. We set the threshold value here (Mw ≥ 6) because the seismo-ionospheric disturbances are sharper for Mw ≥ 6.0. Now the TEC of 6 or more hours for a single day trip out from upper (lower) confidence level would be an abnormal signal. The earthquake days followed by Dst ≤ −50 nT and Kp > 3 are not included in this study as both effects cause changes in the ionosphere. This criteria was used to interrelate GPS TEC anomalies related to global Mw ≥ 5.0 earthquakes from 1998 to 2014.

4. Results and discussion

To define the seismo-ionospheric disturbance related to earthquakes, the TEC values trip out the upper and lower confidence intervals, which are defined as seismo-ionopheric disturbances related to earthquakes by amount equal to the threshold of Mw = 6.0 (Marques de Sa, 2007). The TEC value of more than 6 h for a single day of upper (lower) confidence level has been defined as a seismo-ionospheric disturbance. Fig. 3 shows seismo-ionospheric disturbances related to the Mw = 6.6 earthquake epicenter (56.842°N, 95.911°E) in association with the lower
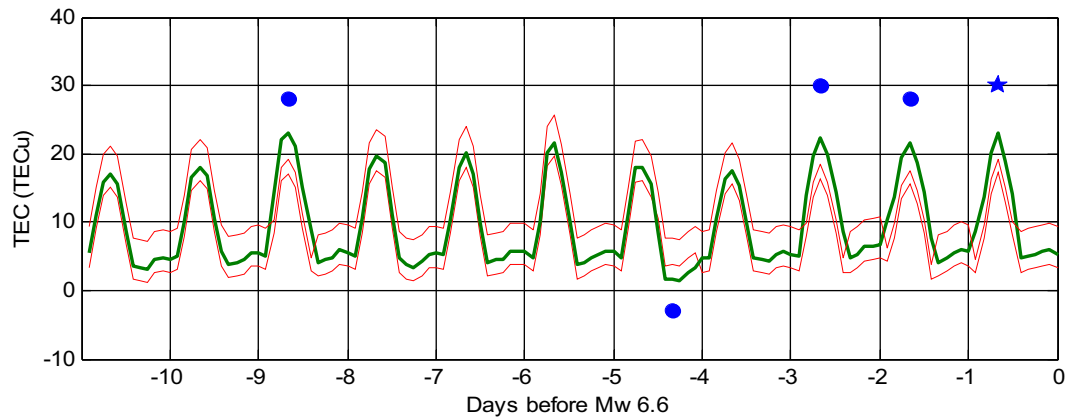
Fig. 3. 10-day seismo-ionospheric disturbances prior to the earthquake with lower (upper) confidential levels. Green bold line and two red lines show lower (upper) TEC confidence levels, respectively. Black star denotes the Mw = 6.6 earthquake epicenter (56.84°N, 95.91°E) on 27 December 2011 and seismo-ionospheric disturbance, respectively. (For interpretation of the references to color in this figure legend, the reader is referred to the web version of this article.)

(upper) confidential level and epicenter as well as pre-earthquake ionospheric anomalies. We have removed the days near the earthquake with Dst ≤ −50 nT and Kp > 3. The TEC variations prior to the Mw = 6.6 earthquake revealed two strong positive anomalies on 2 days −1 and −2 and a negative anomaly on −4 day as shown in Fig. 3. Seismo-ionospheric anomalies in Fig. 3 within 5 days before the Mw = 6.6 earthquake are interpreted in terms of electric field generation and ground motion of earthquake breeding zone.

To examine the suspected hours, we calculated the mean value of TEC for the December 2011 and subtracted the different local times on 25, 26 and 27 December 2011 from the mean value. This showed dissimilarity from others days at UT = 03:00 of 25, 26 and 27 December 2011 as the TEC crest was strongest near the epicenter on these days. Fig. 4a shows the TEC crest near the earthquake epicenter on 25 December 2011. The potential motivation is possibly due to the forthcoming earthquake because as mentioned earlier, the geomagnetic condition was quiet during these days. Fig. 4b illustrates the seismo-ionospheric disturbance on 26 December 2011 prior to the earthquake with a stronger crest of TEC near the epicenter, which may be an indicator of the forthcoming earthquake. Similar variations can be seen in Fig. 4c on 27 December 2011 prior to the earthquake. Strong crest in TEC has been shown in Fig. 4a and b, the variation in TEC at UT = 03:00 is located near the earthquake breeding zone. Since the geomagnetic condition during this period was quiet, the considerable enhancement in TEC on these consecutive days could not be related to space weather and could be a precursor of the Mw = 6.6 earthquake.

In order to investigate the possible pre-earthquake ionospheric anomalies of global earthquakes, the same statistical process has been done for global Mw ≥ 5.0 earthquakes during the period of 1998–2014. The TEC variations within 10 days of the main shock are large. The sudden enhancement in TEC crest is due to forthcoming earthquake (Zakharenkova et al., 2007; Tojiev et al., 2013). Fig. 5 shows the cumulative counts in percentages which are obtained by dividing the number of anomalous days related to earthquakes by the total number of days. We further removed the magnetic storm anomalous days to get all seismo-ionospheric disturbances possibly due to earthquakes. The increase (decrease) percentage was calculated from the cumulative counts by dividing the cumulative count of a single day to sum of cumulative count days. Statistical results used above deviation from normal distribution of TEC due to using Z-percentile instead of t-percentile at $\alpha = 0.05$. Fig. 5 shows an increase in tendency of TEC anomalies with Mw > 6.0 while sharp and regular spikes of anomalous TEC are significant for earthquakes of Mw > 6.5. Days with spikes and regular seismo-ionospheric anomalies are dominant from 4 to 5

days before earthquakes of Mw > 6.0. It has been observed that circulation of energy in the atmosphere and eastward dynamo effect on TEC is due to the seismic activity. Nevertheless, Mw > 6.0 and focal depth <50 km are key elements in causing these primary and short term variations in the ionosphere.

We collected fault classes of earthquakes to check the phenomenon of increase (decrease) percentages of seismo-ionospheric anomalies to these earthquakes. The number of seismo-ionospheric disturbance days is divided by the total number of days multiplied by 100 to get increase (decrease) percentages. Here we performed a statistical analysis for Mw ≥ 6.0 and observed an anomalous pattern with fault related earthquakes from 1998 to 2014. Fig. 6a shows no possible enhancement in TEC caused by normal fault earthquakes in 5 days prior to the earthquakes. As shown in Fig. 6b the variation in increase (decrease) percentage of TEC anomalies is only for Mw ≥ 6.5 earthquakes with oblique fault while the variation in TEC with the other earthquakes is not obvious. It can be seen in Fig. 6c and d that prominent abnormal TEC might be due to strike slip fault and thrusting fault earthquakes in all magnitudes for the period of 1998–2014. Seismo-ionospheric disturbances related to strike slip and thrusting earthquakes are noticeable for Mw6.0–7.0 earthquakes. The Mw ≥ 6.5 was noted in this analysis as an anomaly in GPS TEC for Mw ≥ 6.5 in Fig. 6b–d is sharper than other magnitudes of earthquakes. It is obvious that pre-earthquake ionospheric anomaly for Mw ≥ 6.5 is sharper and more regular than any other magnitude in the statistical analysis carried out for fault classes of different magnitude earthquakes. Astafyeva et al. (2011) have presented possible mechanisms and discussions on seismo-ionospheric disturbance prior to major fault earthquakes around the globe.

In addition, we performed a statistical analysis for Mw ≥ 6.0 and different focal depth earthquakes during 1998–2014 to ensure the variation in TEC related to the focal depth of earthquake because the focal depth is a vital feature of earthquake preparation period. Fig. 7 shows the variation in TEC related to different focal depth earthquakes as it is assumed that the anomaly in TEC is inversely linked to the focal depth of an earthquake. Earthquakes with a focal depth of less than 60 km and Mw ≥ 6 are presumably the root of deviation in ionospheric TEC because such earthquake preparation zones at shallower depth have a gigantic amount of energy. The peak of TEC 5 days before earthquakes in Fig. 7a and b exists with lower focal depth, but for large focal depth, there is no obvious variation in TEC with 5 days before the earthquakes. Horizontal but not steep peak of TEC has been noticed for Mw ≥ 6.0 and focal depth of less than 120 km and 150 km in Fig. 7d and e. Beside magnitude, the focal depth of an earthquake is responsible for discrepancies in TEC. The
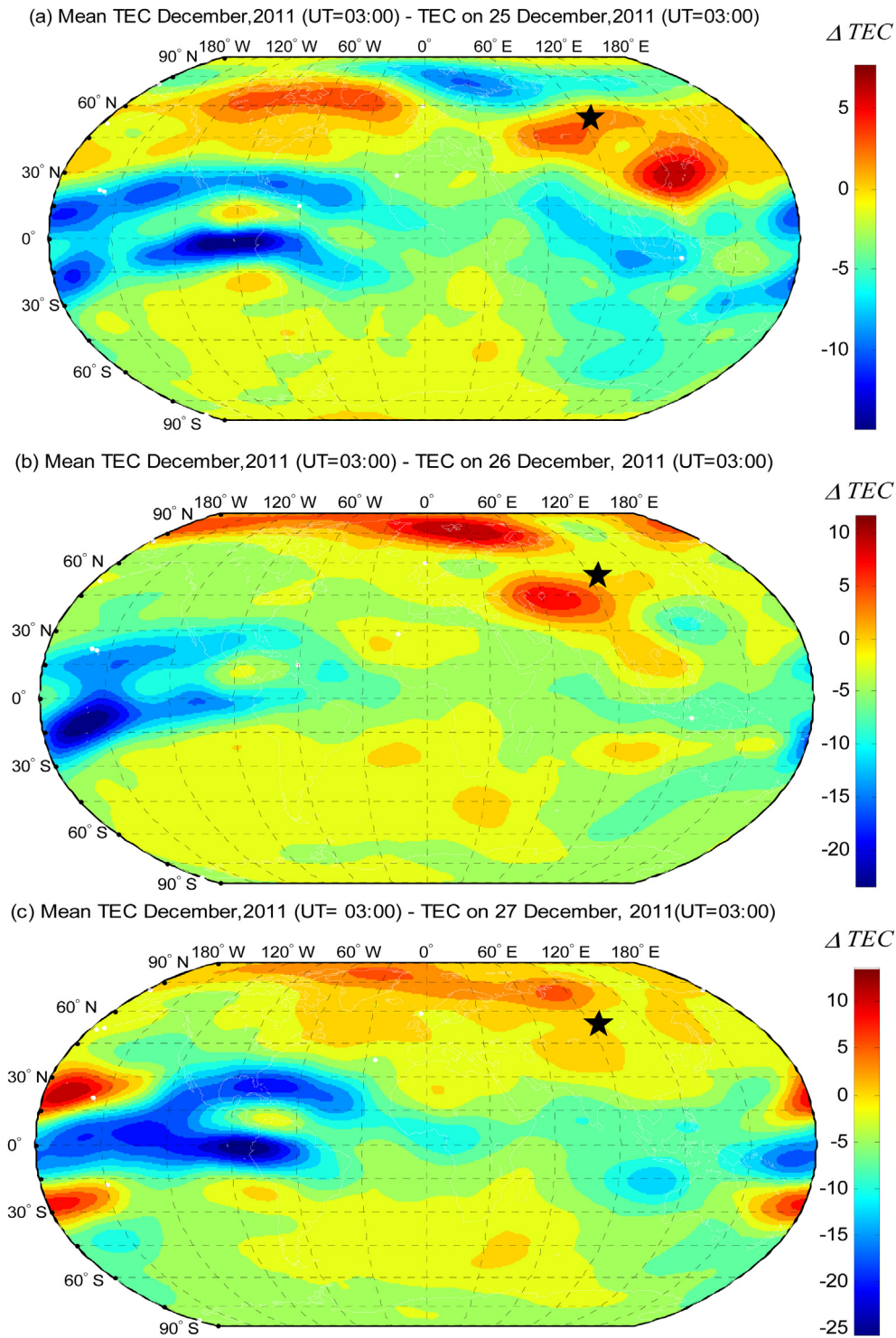
(a) Mean TEC December,2011 (UT=03:00) - TEC on 25 December,2011 (UT=03:00)

(b) Mean TEC December,2011 (UT=03:00) - TEC on 26 December, 2011 (UT=03:00)

(c) Mean TEC December,2011 (UT= 03:00) - TEC on 27 December, 2011(UT=03:00)

Fig. 4. Spatial variation of seismo-ionospheric disturbances related to the Mw = 6.6 earthquake on 27 December 2011. Black star shows the epicenter while (a) mean TEC in December 2011 minus TEC on 25 December 2011, (b) mean TEC in December 2011 minus TEC on 26 December 2011 and (c) mean TEC in December 2011 minus TEC on 27 December 2011.

nighttime variation analysis method concluded that for shallow earthquakes (depth <40 km), the normalized variation and scattering of TEC exhibited a significant increase before earthquakes (Su et al., 2013). These statistical results suggest that propagation anomalies in the ionosphere and shallow earthquakes are directly related. The crest of TEC anomaly can be observed up to ±40° in latitude and ±40° in longitude, showing association with the TEC anomaly in the checked area (Dautermann and Calais, 2007). For describing the status and mechanism of seismo-ionospheric

disturbance (Hayakawa and Molchanov, 2008), the enhanced TEC corresponds that the raised electric field must be in the eastward direction 1–5 days before earthquakes in Japan.

Fig. 8 shows cumulative percentages and relative values of positive and negative anomalies related to global earthquakes of Mw ≥ 5.0. Cumulative percentages have been obtained by dividing the single day TEC anomalies by overall TEC anomalies. The relative values of positive and negative TEC anomalies are expressed as:
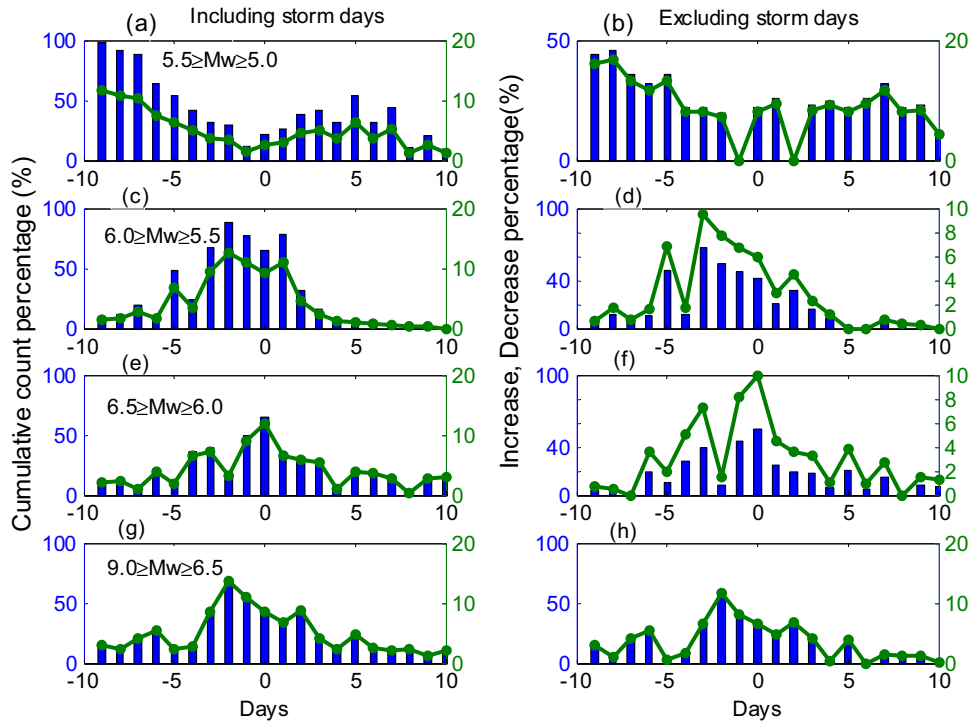
Fig. 5. Cumulative count in percentages (%) and increase (decrease) percentage (%) count for seismo-ionospheric disturbances related to global Mw ≥ 5.0 earthquakes during 1998–2004.
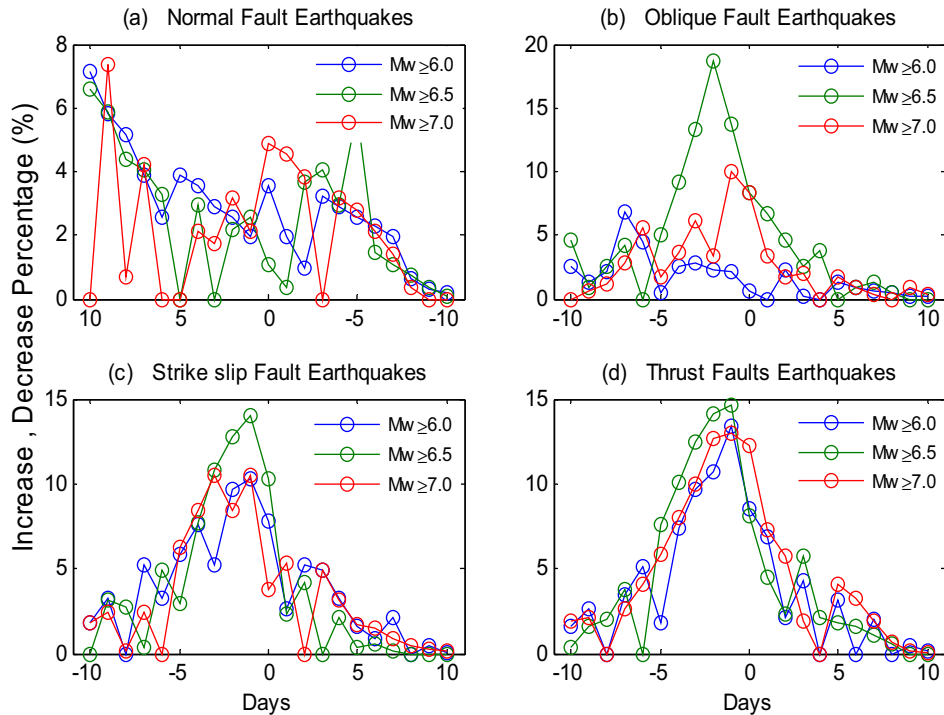

Fig. 6. (a) Increase (decrease) percentages of seismo-ionospheric disturbances for normal faults earthquakes of Mw ≥ 6.0. (b), (c) and (d) are the increase (decrease) percentages of seismo-ionospheric disturbance for oblique fault, strike slip fault and thrust fault earthquakes during 1998–2014, respectively.

$$\text{Relative values} = \frac{\text{TEC Anomaly}_{\text{single day}} - \text{TEC Anomaly}_{\text{mean}}}{\text{TEC Anomaly}_{\text{mean}}}$$

(5)

where TEC Anomaly$_{\text{single day}}$ is the anomaly on a single day and TEC Anomaly$_{\text{mean}}$ is the mean value of 21 days (10 days before (after)

earthquake) positive or negative anomalies. The relative values in Fig. 8 reveal a high ratio (up to 2) of positive anomalies 5 days prior to the global earthquakes, with a tendency similar to cumulative percentages of positive anomalies. The case of negative anomalies is adverse with low ratios (up to −0.5) in relative values. It is interesting to note that positive anomaly days with consistently more
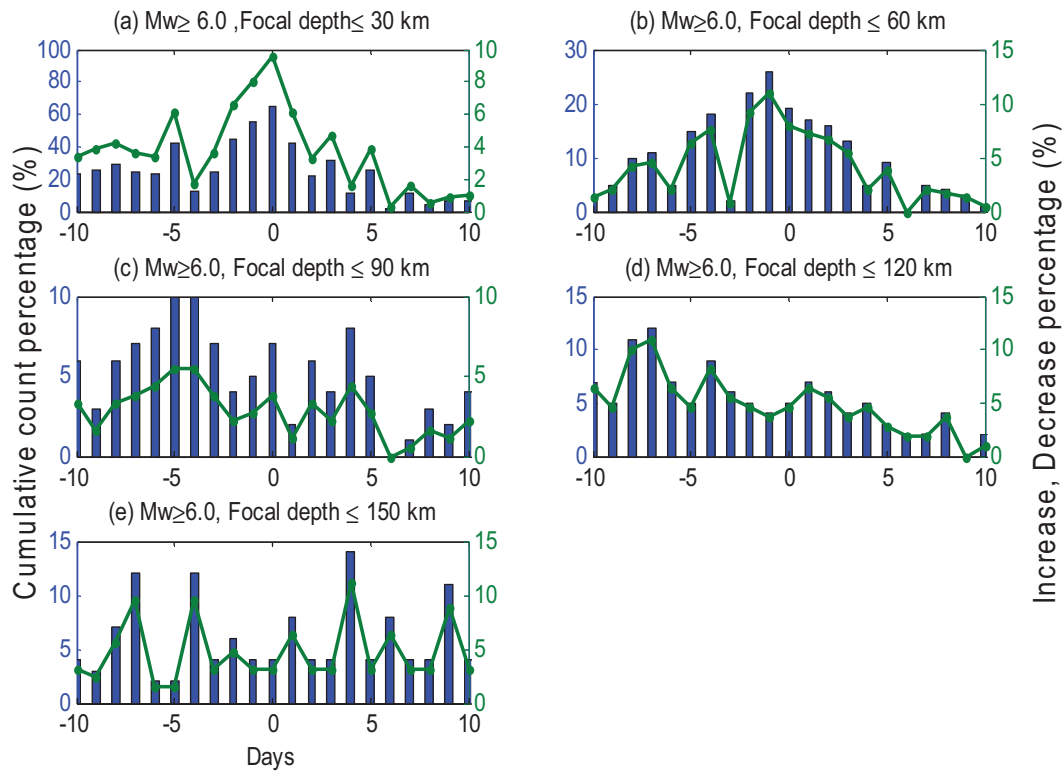
Fig. 7. Cumulative count and increase (decrease) percentages for TEC variations related to the Mw ≥ 6.0 earthquake for different focal depths during 1998–2014.
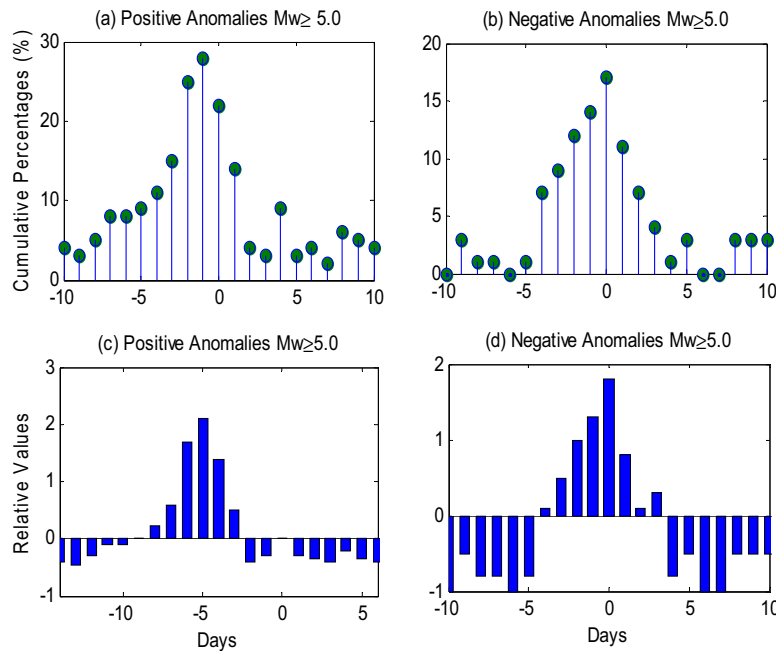

Fig. 8. Cumulative percentages and relative values for global Mw ≥ 5.0 earthquakes during 1998–2014.

than negative anomalies 5 days before global earthquakes suggest that seismo-ionospheric anomalies are generated by earthquakes rather magnetic storms.

5. Conclusion

In this paper, a statistical analysis of seimo-ionospheric anomalies prior to global Mw ≥ 5.0 earthquakes is carried out with a 95% confidence level. Since ionospheric activities with Dst (magnetic storm) and Kp index affect TEC variations, we have removed days with Dst ≤ −50(nT) and Kp > 3. The cumulative count in percentages for seismo-ionospheric disturbances related to earthquakes shows that TEC anomalies for Mw = 6.0 and higher become evident within 5 days prior to earthquakes. The strike slip fault and thrust fault earthquakes regularly cause disturbances in TEC. The anomalous pattern in TEC is regular and sharper for strike slip earthquakes when compared to other classes of fault earthquakes. Oblique fault earthquakes with Mw ≥ 6.5 cause seismo-ionospheric

disturbances and the enhancement in TEC is sharp as strike slip earthquakes. Statistical analysis for Mw ≥ 6.0 and different focal depths show that pre-earthquake TEC anomalies with the focal depth of <50 km are obvious since TEC is susceptible to this large amount of breeding energy. With an increase of focal depth from 60 km, the seismo-ionospheric disturbances related to earthquakes are not clear. In addition, it is understandable that the relative percentage of positive anomalies in TEC is somehow sharper than the relative percentage of negative anomalies. Based on our results, we conclude that the earthquake preparation zone most likely gives birth to seismo-ionospheric anomalies.

Although the percentage of positive anomalies is dominant, the percentages of negative anomalies sporadically appear 5 days before Mw ≥ 5.0 earthquakes all over the globe. Earthquakes are responsible for the generation of pre-seismo-ionospheric disturbance due to sensitivity of the ionosphere to energy evolved by earthquake preparation zone. Here it just shows initial statistical results, which needs more investigations in the future using denser TEC and other observation data, particularly the mechanism of pre-earthquake ionospheric anomalies.

Acknowledgements

References

Afraimovich, E., Ding, F., Kiryushkin, V., Astafyeva, E., Jin, S.G., Sankov, V., 2010. TEC response to the 2008 Wenchuan earthquake in comparison with other strong earthquakes. Int. J. Remote Sens. 31 (13), 3601–3613, http://dx.doi.org/10.1080/01431161003727747.

Astafyeva, E., Lognonné, P., Rolland, L., 2011. First ionospheric images of the seismic fault slip on the example of the Tohoku-oki earthquake. Geophys. Res. Lett. 38, L22104, http://dx.doi.org/10.1029/2011GL049623.

Astafyeva, K., Rolland, L.M., Sladen, A., 2014. Strike-slip earthquakes can also be seen in the ionosphere. Earth Planet. Sci. Lett. 405, 180–193, http://dx.doi.org/10.1016/j.epsl.2014.08.024.

Bolt, B.A., 1999. Earthquake and its After Effects, 4th ed. W.H. Freeman, New York.

Dautermann, T., Calais, E., Haase, J., Garrison, J., 2007. Investigation of ionospheric electron content variations before earthquakes in southern California 2003–2004. J. Geophys. Res. 112, B02106, http://dx.doi.org/10.1029/2006JB004447.

Fatkullin, M.N., Zelenova, T.I., Legen'ka, A.D., 1989. On the ionospheric effects of asthenospheric earthquakes. Phys. Earth Planet. Inter. 57, 82–85.

Fejer, B.G., Scherliess, L., 1995. Time dependent response of equatorial ionospheric electric fields to magnetospheric disturbances. Geophys. Res. Lett. 22, 851–854.

Freund, F., 2000. Time-resolved study of charge generation and propagation in igneous rocks. J. Geophys. Res. 105 (11), 001–011, 019.

Gutenberg, B., Richter, C.F., 1956. Magnitude and energy of earthquakes. Ann. Geofis. 9, 1–15.

Gwal, A.K., Santosh Kumar, J., Gopal, P., Gujar, Y.S., 2011. Study of ionospheric perturbations during strong seismic activity by correlation analysis method. Asian J. Earth Sci. 4, 214–222.

Hayakawa, M., Molchanov, O.A., 2008. Seismo Electromagnetics: Lithosphere–Atmosphere–Ionosphere Coupling. Terra Sci, Tokyo, 477 pp.

Hernandez-Pajares, M., Juan, J.M., Sanz, J., 1999. New approaches in global ionospheric determination using ground GPS data. J. Atmos. Sol. Terr. Phys. 61, 1237–1247.

Jin, S.G., Wang, J., Zhang, H., Zhu, W., 2004. Real-time monitoring and prediction of the total ionospheric electron content by means of GPS observations. Chin. Astron. Astrophys. 28 (3), 331–337, http://dx.doi.org/10.1016/j.chinastron.2004.07.008.

Jin, S.G., Han, L., Cho, J., 2011. Lower atmospheric anomalies following the 2008 Wenchuan Earthquake observed by GPS measurements. J. Atmos. Sol. Terr. Phys. 73 (7–8), 810–814, http://dx.doi.org/10.1016/j.jastp.2011.01.023.

Jin, S.G., Park, P.H., Zhu, W.Y., 2007a. Micro-plate tectonics and kinematics in Northeast Asia inferred from a dense set of GPS observations. Earth Planet. Sci. Lett. 257 (3–4), 486–496, http://dx.doi.org/10.1016/j.epsl.2007.03.011.

Jin, S.G., Cho, J., Park, J., 2007b. Ionospheric slab thickness and its seasonal variations observed by GPS. J. Atmos. Sol. Terr. Phys. 69 (15), 1864–1870, http://dx.doi.org/10.1016/j.jastp.2007.07.008.

Jin, S.G., Luo, O.F., Park, P.H., 2008. GPS observations of the ionospheric F2-layer behavior during the 20th November 2003 geomagnetic storm over South Korea. J. Geod. 82 (12), 883–892, http://dx.doi.org/10.1007/s00190-008-0217-x.

Jin, S.G., Zhu, W.Y., Afraimovich, E., 2010. Co-seismic ionospheric and deformation signals on the 2008 magnitude 8.0 Wenchuan Earthquake from GPS observations. Int. J. Remote Sens. 31 (13), 3535–3543, http://dx.doi.org/10.1080/01431161003727739.

Jin, S.G., van Dam, T., Wdowinski, S., 2013. Observing and understanding the earth system variations from space geodesy. J. Geodyn. 72, 1–10, http://dx.doi.org/10.1016/j.jog.2013.08.001.

Jin, S., Jin, R., Li, J.H., 2014. Pattern and evolution of seismo-ionospheric disturbances following the 2011 Tohoku earthquakes from GPS observations. J. Geophys. Res.: Space Phys. 119, http://dx.doi.org/10.1002/2014JA019825.

Jin, S.G., Occhipinti, G., Jin, R., 2015. GNSS ionospheric seismology: recent observation evidences and characteristics. Earth Sci. Rev. 147, 54–64, http://dx.doi.org/10.1016/j.earscirev.2015.05.003.

Kon, S., Nishihashi, M., Hattori, K., 2011. Ionospheric anomalies possibly associated with M ≥ 6.0 earthquakes in the Japan area during 1998–2010: case studies and statistical study. J. Asian Earth Sci. 41, 410–420.

Le, H., Liu, J.Y., Liu, L., 2011. A statistical analysis of ionospheric anomalies before 736 M6.0+ earthquakes during 2002–2010. J. Geophys. Res. 116, A02303, http://dx.doi.org/10.1029/2010JA015781.

Lin, J.W., 2013. Is it possible to detect earlier ionospheric precursors before large earthquakes using principal component analysis (PCA). Arab. J. Geosci. 6, 1091–1100.

Liu, J.Y., Chen, Y.I., Pulinets, S.A., Tsai, Y.B., Chuo, Y.J., 2000. Seismo-ionospheric signatures prior to M6.0 Taiwan earthquakes. Geophys. Res. Lett. 27, 3113–3116.

Liu, J.Y., Chen, Y.I., Chuo, Y.J., Chen, C.S., 2006. A statistical investigation of preearthquake ionospheric anomaly. J. Geophys. Res. 111, A05304, http://dx.doi.org/10.1029/2005JA011333.

Marques de Sa, J.P., 2007. Applied Statistics Using SPSS. STATISTICA, MATLAB and R Springer, ISBN 978-3-540-71971-7, pp. 85–90.

Molchanov, O.A., Hayakawa, M., 2002. Seismo Electromagnetics and Related Phenomena: History and Latest Results. TERRAPUB, Tokyo, pp. 189.

Pradipta, R., Valladares, C.E., Doherty, P.H., 2014. GPS observation of continent-size traveling TEC pulsations at the start of geomagnetic storms. J. Geophys. Res.: Space Phys. 119, 6913–6924, http://dx.doi.org/10.1002/2014JA020177.

Pulinets, S., Ouzounov, D., 2011. Lithosphere–atmosphere–ionosphere coupling (LAIC) model – an unified concept for earthquake precursors validation. J. Asian Earth Sci. 41, 371–382, http://dx.doi.org/10.1016/j.jseaes.2010.03.005.

Pulinets, S.A., Legen'ka, A.D., Karpachev, A.T., Kochenova, N.A., Migulin, V.V., Orvevski, V.N., Fligel, M.D., 1991. On the Possibility of Earthquakes Prediction on the Basis of Topside Satellite Sounding, 34a. Preprint IZIMIRAN (Russia), pp. 981.

Ryu, K., Parrot, M., Kim, S.G., Jeong, K.S., Chae, J.S., Pulinets, S., Oyama, K.-I., 2014. Suspected seismo-ionospheric coupling observed by satellite measurements and TEC related to the M7.9 Wenchuan earthquake of 12 May 2008. J. Geophys. Res.: Space Phys. 119, http://dx.doi.org/10.1002/2014JA020613.

Sardon, E., Rius, A., Zarraoa, N., 1994. Estimation of the transmitter and receiver differential biases and the ionospheric total electron content from global positioning system observations. Radio Sci. 29, 577–586.

Schaer, S.C., Krankowski, A., 2009. The IGS VTEC maps: a reliable source of ionospheric information since 1998. J. Geod. 83, 263–275, http://dx.doi.org/10.1007/s00190-008-0266-1.

Singh, R.P., Mehdi, W., Gautam, R., Senthil Kumar, J., Zlotnick, J., Kafatos, M., 2010. Precursory signals using satellite and ground data associated with the Wenchuan earthquake of 12 May 2008. Int. J. Remote Sens. 31 (13), 3341–3354.

Su, Y.C., Liu, J.Y., Chen, S.P., Tsai, H.F., Chen, M.Q., 2013. Temporal and spatial precursors in ionospheric total electron content of the 16 October 1999 Mw7.1 hector mine earthquake. J. Geophys. Res.: Space Phys. 118, 6511–6517.

Tojiev, S.R., Ahmedov, B.J., Tillayev, Y.A., Eshkuvatov, H.E., 2013. Ionospheric anomalies of local earthquakes detected by TEC measurements using data from Tashkent and Kitab stations. Adv. Space Res. 52, 1146–1154.

Tsurutani, B.T., Gonzalez, W.D., 1987. The cause of high-intensity long-duration continuous AE activity (HILDCAA): interplanetary Alfven wave train. Planet. Space Sci. 35, 405–412, http://dx.doi.org/10.1016/0032-0633(87)90097-3.

Zakharenkova, I., Shagimuratov, I., Krankowski, A., Lagovsky, A., 2007. Precursory phenomena observed in the total electron content measurements before great Hokkaido earthquake of September 25, 2003 (M = 8.3). Stud. Geophys. Geod. 51 (2), 267–278.

Zolotov, O.V., Namgaladze, A.A., Zakharenkova, I.E., Martynenko, O.V., Shagimuratov, I.I., 2012. Physical interpretation and mathematical simulation of ionospheric precursors of earthquakes at midlatitudes. Geomagn. Aeron. 52, 390–397.